Chinese Science Bulletin

Weak interaction between CH_3SO and HOCl: Hydrogen bond, chlorine bond and oxygen bond

LI ZhiFeng†, LI HongYu, LIU YanZhi, SHI XiaoNing & TANG HuiAn

College of Life Science and Chemistry, Tianshui Normal University, Tianshui 741001, China

B3lyp/6-311++g and mp2/6-311++g** calculations were used to analyze the interaction between CH_3SO and HOCl. Nine (complex A: S1A—S9A) and five (complex B: S4B—S7B and S10B) minima were localized on the potential energy surface of $CH_3SO\cdots HOCl$ complexes at b3lyp/6-311++g** and mp2/6-311++g** computational levels, respectively. The AIM and NBO theories were also applied to explain the nature of the complexes. Bonding energy of complexes A and B corrected with BSSE falls in the ranges of –0.4—–41.4 kJ·mol^{-1} and –6.9—–35.8 kJ·mol^{-1} at mp2/6-311++g** level, respectively. The results show that a novel oxygen bond complex (S6) exists in the system, besides hydrogen bond and chlorine bond. Especially, $S6B_{-F}$, $S6B_{-Br}$ and S7B are blue shifted complexes compared with red shifted S6A, because the electron transfer occurs between LP_1(S8) and σ^*(O5—Cl7), resulting in the increase of O5—Cl7 and the decrease of vibrational frequency. The complex of S10B has characteristics of both red shift and blue shift.**

CH_3SO, HOCl, hydrogen bond, chlorine bond, oxygen bond, NBO, AIM

In the past decades, more and more attention has been paid to the theoretical and experimental investigations on hydrogen bonds due to their important roles in chemistry, physics and biology[1−3]. Nowadays, the following weak interactions have been found: (1) hydrogen bonds, including conventional hydrogen bond X—H···Y and four non-conventional hydrogen bonds[4]; (2) lithium bond[5,6]; (3) cation-π bond[7,8]; (4) halogen bond (D···X—Y, X= Cl, Br or I; Y= C, N, Cl, Br or I)[9]. However, the halogen bonds of D···X—O and S···X—O are seldom reported.

As an important substance in the atmosphere[10], HOCl and its photolytic radicals ·OH and ·Cl all destroy the ozone layer, including its interaction with H_2O (ice) and so on[11,12]. CH_3SO radical can be derived from oxidation of dimethyl sulfide (DMS) in sea water, which can react with a series of small molecular O_2, NO_2 and O_3 resulting in SO_2, and its thermal decomposition also generates SO_2, indicating that CH_3SO may play a critical role in the course of formation of acid rain[13,14]. Li et al.[15] have investigated the stability and isomerizations of CH_3SO at high theoretical level, which showed that CH_3SO is the most stable geometer on the energy surface of isomerizations of CH_3SO. Though the potential surfaces of CH_3SO and HOCl are important, to our best knowledge, there have been no theoretical and experimental studies on their possible interaction. Additionally, the complexes formed between HOCl and CH_3SO can lead to the decrease of effective concentration of HOCl and CH_3SO, which plays an important role in the remission of destruction of the ozone layer and formation of acid rain.

In this work, we investigated the interaction between HOCl and CH_3SO at b3lyp/6-311++g** and mp2/6-311++g** levels. The interaction mechanisms, bond nature and bond characteristics were studied and analyzed by using NBO and AIM theories. The present work exhibits

Received September 4, 2008; accepted April 8, 2009
doi: 10.1007/s11434-009-0477-8
† Corresponding author (email: zflitsnu@163.com)
Supported by the Foundation of Education Committee of Gansu Province (Grant No. 0708-11) and "QingLan" Talent Engineering Funds of Tianshui Normal University

Citation: Li Z F, Li H Y, Liu Y Z, et al. Weak interaction between CH_3SO and HOCl: Hydrogen bond, chlorine bond and oxygen bond. Chinese Sci Bull, 2009, 54: 3014—3022, doi: 10.1007/s11434-009-0477-8

not only hydrogen bond (O···H—O, S···H—O) and chlorine bond (O···Cl—O, S···Cl—O), but also a novel oxygen bond (S···O—X (X = F, Cl, Br)) in the system.

1 Computational details

The structures of monomer and their complexes were optimized at b3lyp/6-311++g** and mp2/6-311++g** levels. on the basis of optimized geometries, the wave functions of NBO and AIM were obtained by using mp2/ 6-311++g** method. The interaction energy of complexes **A** and **B**, with BSSE correction, was calculated at mp2/6-311++g** level. In addition, the interaction energy of complex **B** was verified by using ccsd(t)/ 6-311++g**//mp2/6-311++g** method. The AIM calculations and NBO analyses were carried out using the AIM2000 program and the NBO5.0 package. All the other calculations were performed with the Gaussian 03 program. The BSSE was evaluated using the counterpoise method of Boys and Bernardi[16].

2 Results and discussion

2.1 Structures and interaction energy

Both S and O atoms can act as the active site of proton-acceptor, and they can interact with the H6 atom because S and O possess the lone pair electrons. NPA analysis shows that NPA charge of the Cl7 atom in monomer HOCl is positive (NPA charge: 0.200). Therefore, Cl7 can also serve as a proton-donor atom and interact with the active atoms of S and O in CH_3SO, forming the halogen bond complexes. Nine complexes of **S1A**—**S9A** obtained at b3lyp/6-311++g** level are exhibited in Figure 1, while the vibration frequency, bond change and interaction energy are shown in Table 1. In complexes **S1A**—**S5A**, the major interaction between fragments HOCl and CH_3SO is O···H—O bond, including two weaker interactions of O···H—C and Cl···H—C. As for complexes **S7A**—**S9A**, the halogen bonds of O··· Cl—O and S···Cl—O are important. It is worth noting that a novel weak interaction of S···O—Cl was found in complex **S6A**.

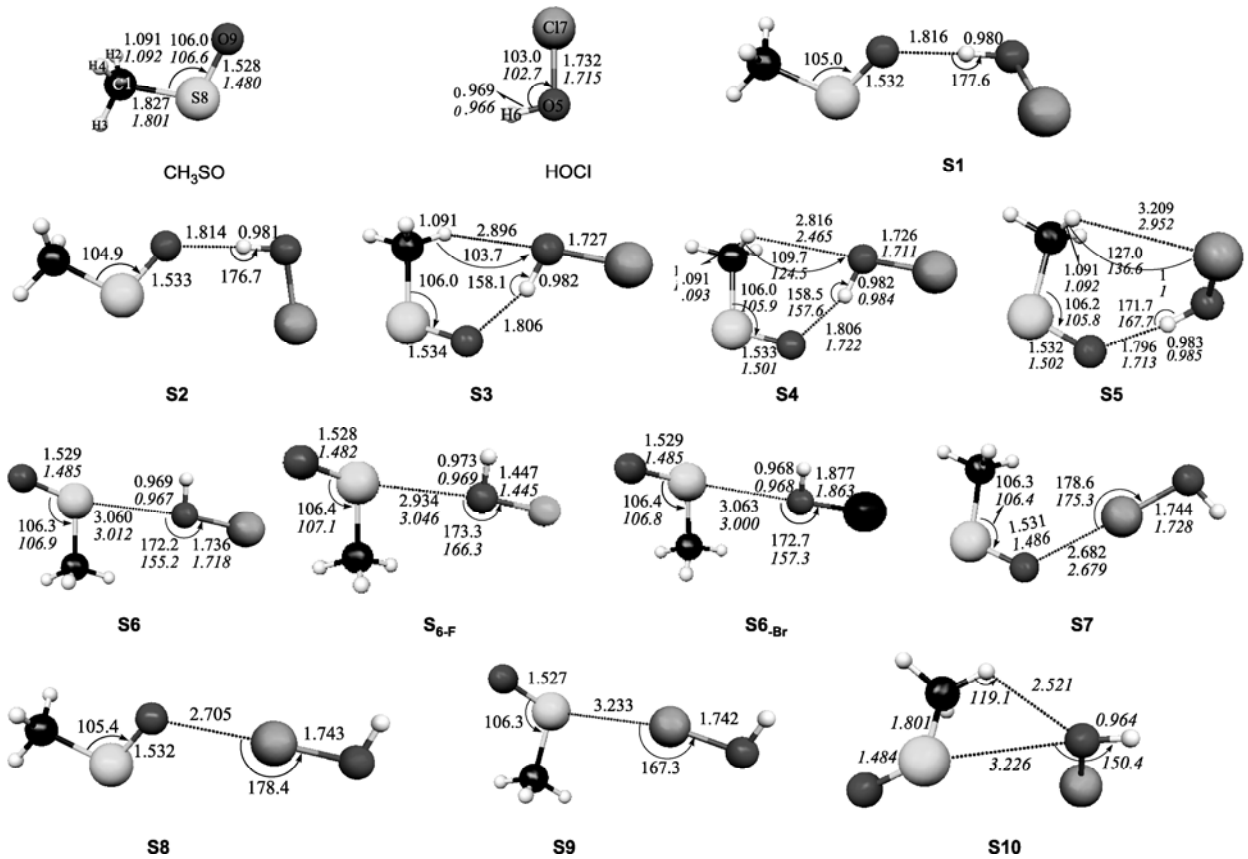

Figure 1 Optimized geometries of complexes at b3lyp/6-311++g** and mp2/6-311++g** (italic parameters) levels (bond length: $\times 10^{-1}$ nm, bond angle: (°).

Theoretical calculations and analysis show that this novel S···O—Cl bond is reasonably termed "oxygen bond" because the S···O—Cl bond exhibits similar properties as the hydrogen bond. In order to have an insight into the generality of oxygen bond, the complexes **S6A**$_{\text{-F}}$ (S···O—F) and **S6A**$_{\text{-Br}}$ (S···O—Br) between CH_3SO and HOF as well as CH_3SO and HOBr were optimized, and the results show that they are similar to complex **S6A**, which further verified that the oxygen bond exists on the potential surface of CH_3SO and HOCl and its existence may be general.

As shown in Figure 1, the parameters of fragment CH_3SO, and especially angles ∠C1S8O9 of external complexes **S1A**, **S2A** and **S8A** are greatly changed compared with the internal complexes of **S3A**, **S4A**, **S5A** and **S7A**. However, in external complexes of **S6A** and **S9A**, the S atoms act as electron-donor atoms, in which the angles of ∠C1S8O9 are almost invariable. In complexes of **S1A**, **S2A**, **S6A**, **S7A** and **S8A**, the weak interaction angles are close to 180°, implying that the hydrogen bond, halogen bond and oxygen bond in the system are all linear bonds, besides, the bond angles of O···H—O have a large deviation from 180° in complexes **S3A**—**S5A**. The binding distance of O9···H6—O5 in complexes is shorter than the sum of the van der Waals radii for one C atom and one H atom (0.26 nm) and longer than the sum of their covalent radii (0.111 nm), suggesting that the hydrogen bond complexes are formed. It is noteworthy that the bond lengths of chlorine bonds (O9···Cl7—O5, S8···Cl7—O5) and novel oxygen bonds (S···O—F, S···O—Cl, S···O—Br) are also between their corresponding sum of covalent radii (0.173, 0.203 and 0.178 nm) and that of van der Waals radii (0.32, 0.365 and 0.325 nm), respectively. Meanwhile, we found that the binding distances of S···O—F, S···O—Cl and S···O—Br increased successively at the b3lyp/6-311 ++g** level. In addition, the weaker interactions of O···H—C and Cl···H—C exist in complexes **S3A**—**S5A,** because their bond lengths are slightly greater than their corresponding sum of the van der Waals radii 0.26 nm and 0.30 nm. Because these secondary hydrogen bonds exist [17], the hydrogen bonds O···H—O in complexes **S3A**—**S5A** deviate from linear direction and the twisted six-membered or five-membered rings form.

Limited by method, we could not obtain interaction energy of two hydrogen bonds in **S3A**, **S4A** and **S5A**, while the total interaction energy could be calculated separately. Actually, it can be considered that total interaction energy of **S3A**, **S4A** and **S5A** obtained by using Boys method was equal to the interaction energy of their corresponding O9···H6—O5 bonds because the strength of O5···H—C and Cl7···H—C is weaker than that of the major hydrogen bonds of O9···H6—O5 (for further discussion, refer to the NBO analysis in Section 2.2). As can be seen from Table 1, the interaction energy of complexes **S1A**—**S5A** is almost equal (in the range of –37.8 — –41.4 kJ·mol^{-1}), and as the O5—H6 bond is elongated, the vibration frequency decreases and finally the red-shifted interaction O···H—O is formed; in complex **S6A**, the O5—Cl7 bond increased by 0.0004 nm and its vibration frequency was red-shifted by 23.0 cm^{-1} compared with that in monomer HOCl, and further the red-shifted oxygen bond (S···O—Cl) formed. The interaction energy of oxygen bond S···O—X (X=F, Cl, Br) falls in the range of –3.7 — –9.4 kJ·mol^{-1}. **S7A**—**S9A** are red-shifted halogen bond (X···Cl—O(X= O, S)) complexes, and the vibration frequency of Cl—O bonds decreased along with their length increasing. Interestingly, the interaction energy of S···Cl—O in **S9A** is the smallest (–0.4 kJ·mol^{-1}) among the complexes **S7A**—**S9A**. The interaction energy of halogen bond, and S···Cl—O is less than that of hydrogen bond and O···Cl—O bonds, respectively. In conclusion, the interaction energy of oxygen bond was in the interaction energy range of halogen bonds O···Cl—O and S···Cl—O. Although the hydrogen bonds in the system are much stronger than those of halogen bond and oxygen bond, they also belong to the weaker interaction because their interaction energy is little.

The system was also studied by using mp2/6-311 ++g** (Figure 1) method because bizarre results are often obtained if the b3lyp is used to study weaker interactions. Calculation results show that the complexes **S4B**—**S7B** obtained at mp2/6-311++g** level are corresponding to **S4A**—**S7A,** respectively. **S10B** is an interesting structure whose existence is predicted only in calculations with mp2/6-311++g** method. As shown in Figure 1 and Table 1, compared to the monomers, the parameters change tendency of complexes is similar at mp2/ 6-311++g** and b3lyp/6-311++g** levels, for example (an exception is ∠C1S8O9 in complexes of **S4**,

Table 1 Bond length differences (Δr: $\times 10^{-1}$ nm), frequency shift (Δv: cm^{-1}) and interaction energy (E^{BSSE}: $kJ \cdot mol^{-1}$)[a)]

Complexes	$\Delta r_{(O5\text{-}H6)}$	$\Delta v_{(O5\text{-}H6)}$	$\Delta r_{(O5\text{-}Cl7)}$	$\Delta v_{(O5\text{-}Cl7)}$	E^{BSSEa}	E^{BSSEb}	E^{BSSEc}
S1A	0.011	–225.1	—	—	–37.8	—	—
S2A	0.012	–232.3	—	—	–38.6	—	—
S3A	0.013	–259.1	—	—	–41.4	—	—
S4A	0.013	–262.0	—	—	–41.0	—	—
S5A	0.014	–276.4	—	—	–40.9	—	—
S6A	—	—	0.012^{HOF}, 0.004, 0.005^{HOBr}	-83.6^{HOF}, –23.0, -19.7^{HOBr}	-3.7^{HOF}, –8.6, -9.4^{HOBr}	—	—
S7A	—	—	0.012	–27.1	–15.4	—	—
S8A	—	—	0.011	–21.0	–13.3	—	—
S9A	—	—	0.01	–35.4	–0.4	—	—
S4B	0.018	–343.8	—		—	–35.8	–27.1
S5B	0.019	–351.0	—		—	–35.4	–26.6
S6B	—	—	0.014^{HOF}, 0.003, 0.003^{HOBr}	836.3^{HOF}, –0.8, 38.0^{HOBr}	—	-5.3^{HOF}, –7.7, -9.0^{HOBr}	-5.0^{HOF}, –6.4, —
S7B	—	—	0.013	24.6	—	–13.6	–9.3
S10B	0.004[b)]	–2.0[b)]	–0.002[c)]	13.8[c)]	—	–6.9	–5.7

a) E^{BSSEa} denotes the energies obtained at mp2/6-311++g**//b3lyp/6-311++g** level; E^{BSSEb} and E^{BSSEc} denote the energies obtained at mp26-311++g**// mp2/6-311++g** and ccsd(t)/6-311++g**//mp2/6-311++g** level, respectively; b) S8-O9 bond; c) C1-H3 bond.

S5 and **S7**), O5—H6 bond is less elongated in **S4** than that in **S5,** and also **S4** and **S5** are both red-shifted complexe. Generally, **S6** and **S7** are both the red-shifted complexes because the O5—Cl7 bond increased in complexes compared with monomer HOCl at mp2/6-311++g** and b3lyp/6-311++g** levels. However, from Table 1, the frequency analysis at mp2/6-311++g** level confirms that the stretching frequencies of O5—Cl7 bond in **S6B**$_{\text{-F}}$, **S6B**$_{\text{-Br}}$ and **S7B** are blue-shifted along with its elongations. **S10B** contains a pair of intermolecular interactions O···S—O and O···H—C, which leads to S8—O9 and C—H3 bonds elongation, shortened by 0.0004 nm and 0.0002 nm, respectively. The stretching frequencies of S8—O9 and C—H3 are red shifted (2.0 cm^{-1}) and blue shifted (13.8 cm^{-1}). The complex of **S10B** has both red and blue shifts. As shown in Table 1, the interaction energy (E^{BSSEa}, E^{BSSEb} and E^{BSSEc}) at three computational levels is well consistent with each other.

For the sake of completeness, the rotational constants for the monomers and the complexes are also listed in Table 2 at mp2/6-311++g** computational level. The five complexes are asymmetric rotors and behave like prolate rotors, with $I > II \approx III$. The computed rotational constants for hypochlorous acid can be compared well with the experimental values [18].

Table 2 Rotational constants (in GHz) for HOCl, CH_3SO, **S4B**—**S7B** and **S10B** complexes

Complexes	I	II	III
HOCl[a)]	610.81	14.75	14.41
CH_3SO	28.13	8.50	6.81
S4B	7.32	1.03	0.94
S5B	5.20	1.36	1.27
S6B	9.44	0.88	0.83
S7B	7.83	1.06	0.95
S10B	5.79	1.12	1.06

a) The experimental values for HOCl are 613.38, 15.12 and 14.73 GHz[18].

2.2 Natural bond orbital (NBO) analysis

The formation mechanisms of hydrogen bond, halogen bond and oxygen bond between CH_3SO and HOCl were studied by using NBO theory. The original paper of Alabugin et al.[19] states that red shift and blue shift of H bonds are all determined by balance of hyperconjugation and rehybridization. Table 3 lists the calculated results of complexes **A** and **B** at mp2/6-311++g** level, in which the $\Delta q\{\sigma^*\}$, $\Delta q\{\mathrm{LP}(Y)\}$, $\Delta q(X)$, EDT and Δs/% reflect the characteristics of hyperconjugation and rehybridization.

In hydrogen bond complex **S1A**, the main intermolecular hyperconjugation electron density transfers from $LP_{2,1}(O9)$ to σ* (O5—H6), which directly causes the O5—H6 bond elongation and its stretching frequency is red shift (Figure 2). On the other hand, the $q\{\mathrm{LP}(Y)\}$ and $q\{\sigma^*(O5—H6)\}$ are less and higher by 0.0055 e and

Table 3 NBO analysis at MP2/6-311++g** level

Species	Donor (*i*)				Acceptor (*j*)				$E_{ij}^{(2)}$ (kcal·mol^{-1})	E_j-E_i (a.u.)
	Orbital	sp^n	Δq{LP(*Y*)}	EDT	Orbital	Δq {σ*}	$sp^n(X)$	Δs (%)		
S1A	LP_2(O9)	$sp^{21.39}$	–0.0017	0.0157	σ*(O5—H6)	0.0075	$sp^{2.69}$	3.97	5.57	1.25
	LP_1(O9)	$sp^{0.41}$	–0.0038						2.44	1.74
S2A	LP_2(O9)	$sp^{20.88}$	–0.0018	0.0157	σ*(O5—H6)	0.0050	$sp^{2.69}$	3.77	5.68	1.25
	LP_1(O9)	$sp^{0.41}$	–0.0038						2.45	1.74
S3A	LP_2(O9)	$sp^{99.99}$	–0.0015	0.0191	σ*(O5—H6)	0.0062	$sp^{2.66}$	3.96	4.85	1.20
	LP_1(O9)	$sp^{0.33}$	–0.0055						3.24	1.75
	LP_2(O5)	$sp^{99.99}$	—	—	σ*(C1—H3)	—	—	—	0.03	1.15
S4A	LP_2(O9)	$sp^{99.99}$	–0.0014	0.0190	σ*(O5—H6)	0.0090	$sp^{2.67}$	4.11	4.79	1.20
	LP_1(O9)	$sp^{0.33}$	–0.0056						3.25	1.75
	LP_2(O5)	$sp^{99.99}$	—		σ*(C1—H2)	—	—	—	0.04	1.15
S5A	LP_2(O9)	$sp^{99.99}$	–0.0064	0.0171	σ*(O5—H6)	0.0064	$sp^{2.66}$	4.00	4.71	1.20
	LP_1(O9)	$sp^{0.34}$	–0.0011						3.87	1.76
	LP_3(Cl7)	$sp^{99.99}$	—		σ*(O5—C17)	—	—	0.30	0.10	1.08
S6A	LP_1(S8)	$sp^{0.49}$	–0.0010	0.0044	σ*(O5—C17)	0.0023	$sp^{2.52}$	–0.31	0.19	0.95
	σ(S8—O9)	—	—				—		0.13	0.61
S7A	LP_2(O9)	$sp^{99.99}$	–0.0020	0.0094	σ*(O5—C17)	0.0046	$sp^{7.57}$	0.64	1.45	0.71
	LP_1(O9)	$sp^{0.32}$	–0.0033						1.32	1.27
S8A	LP_2(O9)	$sp^{39.06}$	–0.0029	0.0088	σ*(O5—C17)	0.0040	$sp^{7.54}$	0.40	2.06	0.73
	LP_1(O9)	$sp^{0.36}$	–0.0015						0.75	1.26
S9A	LP_1(S8)	$sp^{0.49}$	–0.0022	0.0131	σ*(O5—C17)	0.0091	$sp^{8.46}$	—	0.61	0.97
	LP_1(Cl7)	$sp^{0.22}$	—		σ*(S8—O9)	0.0004	$sp^{99.99}$	0.01	0.12	0.69
S4B	LP_2(O9)	$sp^{91.46}$	–0.0011	0.0251	σ*(O5—H6)	0.0121	$sp^{2.59}$	4.62	5.72	1.19
	LP_1(O9)	$sp^{0.37}$	–0.0070						4.41	1.73
	LP_2(O5)	$sp^{99.99}$	—		σ*(O5—H6)	—	—	—	0.23	1.16
S5B	LP_1(O9)	$sp^{0.37}$	–0.0079	0.0230	σ*(O5—H6)	0.0125	$sp^{2.60}$	4.51	5.19	1.74
	LP_2(O9)	$sp^{95.24}$	–0.0021						5.14	1.20
	LP_3(Cl7)	$sp^{81.33}$	—	—	σ*(O5—H6)	—	—	—	0.31	1.09
S6B	LP_1(S8)	$sp^{0.54}$	–0.0010	0.0030	σ*(O5—H6)	0.0005	$sp^{11.99}$	–0.08	0.14	0.94
	σ(S8—O9)	—	—				—		0.10	0.63
S7B	LP_1(O9)	$sp^{0.37}$	–0.0030	0.0086	σ*(O5—H6)	0.0060	$sp^{7.34}$	0.45	1.30	1.27
	LP_2(O9)	$sp^{99.99}$	0.0000						0.97	0.71
S10B	LP_1(O5)	$sp^{0.54}$	–0.9993	0.0010	σ*(O5—H6)	0.0003	$sp^{2.79}$	0.35	0.15	1.70
					σ*(O5—H6)	0.0003	$sp^{2.61}$	–0.06	0.11	1.63

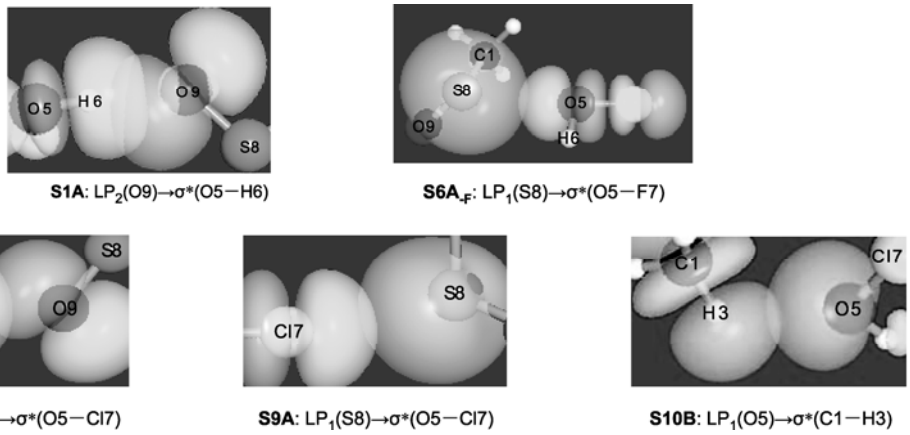

S1A: LP_2(O9)→σ*(O5—H6) **S6A$_F$**: LP_1(S8)→σ*(O5—F7)

S7A: LP_2(O9)→σ*(O5—Cl7) **S9A**: LP_1(S8)→σ*(O5—Cl7) **S10B**: LP_1(O5)→σ*(C1—H3)

Figure 2 Three-dimensional electron transfer characteristics of selected complexes.

0.00745 e than those in free monomers.

Electron density transfer (EDT) from electron-donor CH_3SO (proton-accepted) to electron-accepted HOCl (proton-donor) is 0.0157 e. Compared with LP_1(O9) ($sp^{0.41}$) and LP_2(O9)($sp^{21.39}$), the electron transfer of LP_2 (O9)→σ*(O5－H6) is more effective because the orbital interactions between LP_2(O9) and σ* (O5－H6) overlap head to head. In addition, the orbital energy difference between LP_2(O9) and σ* (O5－H6) is 0.49 a.u, less than that between LP_1(O9) and σ* (O5－H6), which can also cause the electron transfer from LP_2(O9) to σ*(O5－H6) easily and the second order stabilization energy $E_{ij}^{(2)}$ [LP_2(O9)→σ* (O5－H6)] is 3.1 kJ·mol^{-1}, higher than that of $E_{ij}^{(2)}$ [LP_1(O9)→σ * (O5－H6)].

Among 3 interactions of **S3A**－**S5A**, the most important donor-acceptor electron interaction occurred between LP_2(O9) and σ*(O5－H6), which is similar to that in **S1A**. As pointed out above, the weaker secondary hydrogen bonds O⋯H－C and Cl⋯H－C ($E_{ij}^{(2)}$ are about 0.5 kJ·mol^{-1}) also exist in complexes **S3A**－**S5A**, except the O⋯H－O interactions, leading to six or seven-membered circle electron transferring. Maybe for this reason, the $E_{ij}^{(2)}$ [LP_2(O9)→σ*(O5－H6)] in **S1A** and **S2A** is about 3.0 kJ·mol^{-1}, higher than those in interactions of **S3A**－**S5A**.

Complexes **S7A**－**S9A** are chlorine bond interaction, of which **S7A** and **S8A** belong to the kind of O⋯Cl－O and the main electron transfer in them is of LP_2 (O9) →σ*(O5－Cl7). However, in complex **S8A**, the $E_{ij}^{(2)}$ [LP_2(O9)→σ*(O5－Cl7)] is about 2.6 kJ·mol^{-1} higher than that in complex **S7A,** because the overlap of cloud between LP_2(O9) and σ*(O5－Cl7) is more efficient in complex **S8A**. Complex **S9A** can be ascribed to S⋯Cl －O interaction. Generally, the $E_{ij}^{(2)}$ [LP_2(O9)→ σ* (O5－Cl7)] in **S9A** is higher than that in **S7A** and **S8A** in that the donor property of S atom is stronger than that of O atom, which leads to the electron transfer easily between LP_2(O9) and σ*(O5－Cl7). However, according to the analysis, the main orbital interaction between fragments HOCl and CH_3SO in **S9A** is of σ*(S8－O9) and σ*(O5－Cl7), of which the most important electron transfer occurred between LP_1(S8) and σ*(O5－Cl7) ($E_{ij}^{(2)}$ only 2.6 kJ·mol^{-1}), maybe due to the electron transferring from LP_1(Cl7) to σ*(S8－O9), which can offset LP_1(S8)→σ*(O5－Cl7) transferring partly. In addition, from the angle of NPA charge, the NPA charges of S and O atoms are positive (0.7197) and negative (–0.6303) in monomer CH_3SO respectively. In monomer HOCl, the NPA charge of Cl is 0.1977, unfavorable to form chlorine bond because the involved interaction atoms all held positive charge, against the nature of halogen bond.

In addition, a novel weak interaction in red-shifted complex **S6A** exists in CH_3SO-HOCl interactions, in which the main orbital interactions are of LP_1(S8)→σ* (O5－Cl7) and σ(S8－O9)→σ*(O5－Cl7), leading to the increase of the charge of σ*(O5－Cl7) by 0.0023 e and the O5－Cl7 is elongated by 0.0004 nm. Although LP_1(S8) ($sp^{0.49}$) and σ*(O5－Cl7) overlap head to head, the overlap is efficient partially, resulting in that the $E_{ij}^{(2)}$ [LP_1(S8)→σ*(O5－Cl7)] is only 0.8 kJ·mol^{-1}.

It is worth noting that redistribution of electron density leads to rehybridization accruing (Table 3). For hydrogen bond complexes **S1A**－**S5A**, the *s* of O5 hybrid in σ(O5－H6) increased by more than 3.77%, and for halogen interactions **S7A**－**S9A**, the *s* of O5 hybrid in σ(O5－Cl7) increased by no more than 0.40%. As described in Table 3, there is a positive correlation between the strength of hyperconjugation and rehybridization, and in the same complex, the hyperconjugative interaction dominates compared with rehybridizations interaction. Interestingly, the Δ*s* of X7 hybrid in σ(O5－X7) are –0.31%, 0.70%, and –0.16% for **S6A**, **S6A**$_{\text{-F}}$, and **S6A**$_{\text{-Br}}$, respectively, suggesting that the *s* of X7 hybrid decreased with F→Cl→Br sequence.

Meanwhile, for hydrogen bond (**S1A**－**S5A**) and halogen bond (**S7A**－**S9A**) complexes, the larger the *p* characters of X hybridization in H－X/Cl－X bond is, the smaller the absolute interaction energy with complexes will be, that is, the strength is stronger and the absolute interaction energy is greater while the *s* of X in hybrid orbital increases. For example, the hybrid modes of O5 atom in five complexes **S1A**－**S5A** are almost equal ($sp^{2.66–2.69}$), leading to that their interaction energy is also close to each other (about –40 kJ·mol^{-1}). However, for complex **S9**, the p of O5 are about 89.4%, larger than those in **S7A** and **S8A** complexes, and the in-

teraction energy of **S9** is only –0.4 kJ·mol^{-1}, which is smaller than that of **S7A** and **S8A**.

As also can be seen from Table 3, the analysis results of **A** and **B** complexes by using NBO are almost consistent. The NRT[20] results show that the weak interaction properties between bonding atoms are completely ionic (limited by space, the relative calculated results are not listed here).

2.3 Analysis of atoms in molecules (AIM)

Topological parameters are helpful to understanding the mechanism of weak interaction, thus the Bader theory[21, 22] was applied here to characterize the interactions between CH_3SO and HOCl at the mp2/6-311++g** level. When the AIM theory is used to study the weak interaction, three important parameters and eight criteria are involved. Parameters (1): The electron densities $\rho(\boldsymbol{r}_c)$ have positive correlation with bond strength, that is, the $\rho(\boldsymbol{r}_c)$ is bigger(smaller), and the bond strength is stronger (weaker); parameters (2): Laplacians $\nabla^2\rho(\boldsymbol{r}_c)$ reflect the characters of bond, and while the $\nabla^2\rho(\boldsymbol{r}_c)>0$, the bond holds the ionic properties, whereas the bond possesses the covalent features; parameters (3): When ellipticity $\varepsilon = \lambda_1/\lambda_2-1$ the larger the value of ε, the stronger the π characters of bond. The $\varepsilon\rightarrow 0$ indicates that the bond holds the typical σ property. Eight topological criteria for the existence of hydrogen bonding interactions were indicated by Popelier et al.[23]. Among them three are most often applied: (1) The bond paths and bond critical points (BCP) exist between the interaction atoms; (2) the $\rho(\boldsymbol{r}_c)$ value at BCP should be within the range of 0.002－0.034 a.u.; (3) the $\nabla^2\rho(\boldsymbol{r}_c)$ value at BCP should be within the range of 0.024－0.139 a.u. and so on.

According to the AIM, the molecular graph is intuitionistic for the topological property of electron density, which can also display the structure of bond in the system. Figure 3 detects the selected molecular graphs of monomers and complexes**,** which indicate that there are two kinds of critical points, namely, ring critical points ((3, +1), RCP) and bond critical points ((3, –1), BCP) existing in corresponding complexes. The parameters values in Figure 3 are in the order of electron density $\rho(\boldsymbol{r}_c)$, Laplacians $\nabla^2\rho(\boldsymbol{r}_c)$ and ellipticity ε at the corresponding bonds. On the basis of the values from $\rho(\boldsymbol{r}_c)$ and $\nabla^2\rho(\boldsymbol{r}_c)$, the weak interactions could be divided into 3 groups, the first group with the $\rho(\boldsymbol{r}_c)$ and $\nabla^2\rho(\boldsymbol{r}_c)$ in the range of 0.0313－0.0336 a.u., and 0.1166－0.1198 a.u. respectively, corresponding to the hydrogen bonds (O···H－O) complexes **S1A**－**S5A**; the second kind is chlorine bond (X···Cl－O(X= O, S)) complexes of **S7A**－**S9A**, and the values of $\rho(\boldsymbol{r}_c)$ and $\nabla^2\rho(\boldsymbol{r}_c)$ are in the range of 0.0112－ 0.0189 a.u. and 0.0374－0.0727 a.u. The oxygen bond interaction (**S6A$_{\text{-F}}$**: S···O－F, **S6A**: S···O－Cl and **S6A$_{\text{-Br}}$**: S···O－Br) could be put into the third group, and their $\rho(\boldsymbol{r}_c)$ and $\nabla^2\rho(\boldsymbol{r}_c)$ values are the smallest among the three groups, which is in the range of 0.0098 － 0.0126 a.u. and 0.0350－0.0506 a.u., respectively. These results are inconsistent with the classification based on the interaction energy in Section 2.1. Meanwhile, it can be seen from Figure 3 that the $\rho(\boldsymbol{r}_c)$ of bond H2···O5 in **S3A**, that of bond H4···O5 in **S4A** and that of bond H4···Cl7 in **S5A** are all close to the lower limit of Popelier (0.002 a.u.), and also their $\nabla^2\rho(\boldsymbol{r}_c)$ are the smallest among the nine interactions, which indicates that the interactions of H2···O5, H4···O5 and H4···Cl7 are all the weakest in complexes **S3A**－**S5A**, respectively. Typically, in nine interactions, the values of $\nabla^2\rho(\boldsymbol{r}_c)$ at BCP of O···H－O, X···Cl－O(X = O, S) and S···O－H are all positive, which demonstrates that all the hydrogen bond, chlorine bond and oxygen bond possess the characters of ion. Meanwhile, although ellipticity of nine complexes is all close to zero and the σ characters of bond are principal, the ellipticity of **S2A**－**S9A** is about three times higher than that of **S1A**, because three atoms of HOCl and C, S, O atoms in CH_3SO are in either the same plane or the ring formed in the interactions of **S2A**－**S9A**. Based on the above reasons, large π bonds are formed easily in **S2A**－**S9A**, as a result, the π characters of weak bond in **S2A**－**S9A** are much higher than those in **S1A.** Interestingly, the ellipticity of oxygen bond S···O－H is the biggest among the nine complexes. In addition, in the same type of complexes of **S6A$_{\text{-F}}$**, **S6A** and **S6A$_{\text{-Br}}$**, the ε (S···O－F) is the smallest and the ε (S···O－Br) is the biggest, which is consistent with the interaction energy of **S6A$_{\text{-F}}$**, **S6A** and **S6A$_{\text{-Br}}$** discussed in Section 2.1.

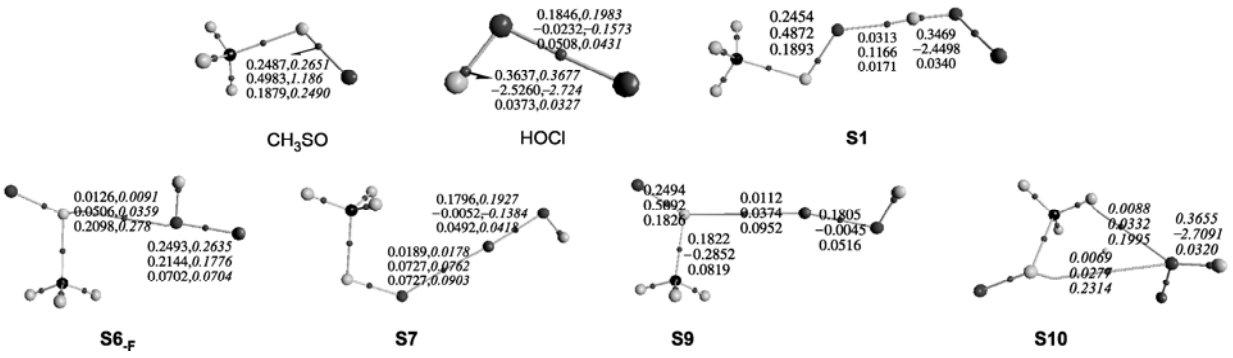

Figure 3 Selected molecular graphs of complexes and topological parameters (italic parameters corresponding to complex **B**).

3 Conclusions

Hybrid density functional (b3lyp) and second-order perturbation (mp2) methods have been employed to study the interactions between HOCl and CH_3SO. Further more, the NBO theory is performed to discuss the electron transfer density (EDT), the NRT order, hyperconjugation ($E^{(2)}$) and rehybridizations in the system. The topological characters of complexes are investigated by AIM theory in detail.

There are three kinds of red-shifted weak interactions between CH_3SO and HOCl at b3lyp/6-311++g** level, including five hydrogen bond complexes (**S1A**−**S5A)**, three halogen bond complexes (**S7A**−**S9A)** and one novel oxygen bond complex (**S6A)**. Moreover, the oxygen bond complexes **S6A**$_{\textbf{-F}}$ and **S6A**$_{\textbf{-Br}}$ are formed and they are similar to complex **S6A,** while CH_3SO interacts with HOF and HOBr. Five minima (**S4B**−**S7B**, **S10B**) are located on the potential energy surface between CH_3SO and HOCl at mp2/6-311++g** computational level, in which the complexes **S4B**, **S5B** and **S6B** are all red-shifted and they are similar to complexes **S4A**, **S5A** and **S6A** respectively. For oxygen bond (**SB6**$_{\textbf{-F}}$, **SB6**$_{\textbf{-Br}}$) and halogen bond (**S7B)** complexes, however, the abnormal blue-shifted complexes are formed along with the elongation of corresponding O−X(X=F, Br) and Cl−O bonds. Complex **S10B** has the two-sided characteristics of red and blue shifts.

The absolute interaction energy decreased in the following sequence: $E^{\mathrm{BSSEa}}_{\text{hydrogen bond}}$ (–37.8— –41.4 kJ·mol^{-1}) > $E^{\mathrm{BSSEa}}_{\text{hydrogen bond}}$ (−13.3, −15.4 kJ·mol^{-1})> $E^{\mathrm{BSSEa}}_{\text{hydrogen bond}}$ (–3.7— –9.4 kJ·mol^{-1}), except that the $E^{\mathrm{BSSEa}}_{\mathrm{S\cdots Cl-O}}$ (only –0.4 kJ·mol^{-1}) is smaller than that of oxygen bond. And for $E^{\mathrm{BSSEa,b,c}}_{\mathrm{HOBr}}$, $E^{\mathrm{BSSEa,b,c}}_{\mathrm{HOCl}}$ and $E^{\mathrm{BSSEa,b,c}}_{\mathrm{HOF}}$, the sequence of increase is in the order of $E^{\mathrm{BSSEa,b,c}}_{\mathrm{HOBr}} < E^{\mathrm{BSSEa,b,c}}_{\mathrm{HOCl}} < E^{\mathrm{BSSEa,b,c}}_{\mathrm{HOF}}$, which is consistent with the electronegativity of halogen atoms.

The characters of weak interaction in complexes **A** and **B** are ionic mainly according to the results of NRT bond order and Laplacians $\nabla^2\rho(\boldsymbol{r}_c)$ by NBO and AIM analysis, respectively.

AIM analysis shows that interatomic paths and bond critical points BCP are located between interaction atoms in hydrogen bond, halogen bond and oxygen bond complexes. For complex **A**, electron density $\rho(\boldsymbol{r}_c)$ and Laplacin $\nabla^2\rho(\boldsymbol{r}_c)$ in hydrogen bond, chlorine bond and oxygen bond are 0.0038−0.0336 a.u., 0.0112−0.0189 a.u., 0.0098−0.0126 a.u. and 0.0113−0.1198 a.u., 0.0374−0.0762 a.u., 0.0350−0.0506 a.u., respectively. For complex **B**, $\rho(\boldsymbol{r}_c)$ and $\nabla^2\rho(\boldsymbol{r}_c)$ are 0.0054−0.0384 a.u., 0.0178 a.u., 0.0091−0.0116 a.u. and 0.0191−0.1537 a.u., 0.0762 a.u., 0.0359−0.0422 a.u. in interaction hydrogen bond, chlorine bond and oxygen bond respectively.

The results of this paper, especially the investigation on the novel oxygen bond weak interaction in detail, might be helpful to not only finding new binding sites and high efficient probe molecules but also developing nonbonding interaction theory. Although the oxygen bond interaction has been investigated in this paper, its nature and universality in experiment and theory might be material. Moreover, the criteria of oxygen bond interaction must be further discussed.

1 Hobza P, Sponer J. Structure, energetics, and dynamics of the nucleic acid base pairs: nonempirical *ab initio* calculations. Chem Rev, 1999, 99: 3247－3276

2 Li Y B, Zeng Q D, Wang Z H, et al. Constructing supramolecular nanostructure by hydrogen-bonding. Chinese Sci Bull, 2008, 53: 1613－1616

3 Aloisia S, Franscisco J S. Radical-water complexes in earth's atmosphere. Acc Chem Res, 2000, 33: 825－830

4 Grabowski S J. High-level *ab initio* calculations of dihydrogen-bonded complexes. J Phys Chem A, 2000, 104: 5551－5557

5 Kollman P A, Liebman J F, Allen L C. Lithium bond. J Am Chem Soc, 1970, 92: 1142－1150

6 Vila A, Vila E, Mosquera R A. Topological characterization of intermolecular lithium bonding. Chem Phys, 2006, 326: 401－408

7 Ma J C, Dougherty D A. The cation-π interaction. Chem Rev, 1997, 97: 1303－1324

8 Cheng J G, Zhu W L, Wang Y L, et al. The open-close mechanism of M2 channel protein in influenza A virus: A computational study on the hydrogen bonds and cation-p interactions among His37 and Trp41. Sci China Ser B-Chem, 2008, 51: 768－775,

9 Dumas J M, Gomel M, Guerin M. Molecular Interactions Involving Organic Halides . New York: John Wiley & Sons Ltd, 1983. 985－1020

10 Leu M T. Laboratory studies of sticking coefficients and heterogeneous reactions important in the antarctic stratosphere. Geophys Res Lett, 1988, 15: 17－20

11 Solimannejad M, Alkorta I, Elguero J. Stabilities and properties of O_3-HOCl complexes: A computational study. Chem Phys Lett, 2007, 449: 23－27

12 Zhou Y F, Liu C B T. Theoretical study of HOCl adsorption on ice surface. J Phys Chem Sol, 1999, 60: 2001－2004

13 Turnipseed A A, Ravishankara A R. Dimethylsulfide: Oceans, atmosphere and climate. In: Restelli G., Ed. Proceeding of the International Symposium Held in Belgirate, Italy, 13-15 October, 1993. New York : Kluwer Academic, 1992. 185

14 Ravishankara A R, Rudich Y, Talukdar T, et al. Oxidation of atmospheric reduced sulphur compounds: Perspective from laboratory studies. Philos Trans R Soc London Ser B, 1997, 352: 171－182

15 Li X Y, Fan H M, Meng L P, et al. Theoretical investigation on stability and isomerizations of CH_3SO isomers. J Phys Chem, 2007, 111: 2343－2350

16 Boys S F, Bernardi F. Calculation of small molecular interactions by differences of separate total energies. Some procedures with reduced errors. Mol Phy, 1970, 19: 553－556

17 Wu D, Li Z R, Hao X Y. An *ab initio* theoretical prediction: An antiaromatic ring π-dihydrogen bond accompanied by two secondary interactions in a "wheel with a pair of pedals" shaped complex FH···C4H4···HF. J Chem Phys, 2004, 120: 1330－1335

18 NIST Standard Reference Database No. 69, March 2003 ed. http://webbook.nist.gov/chemistry, 2005

19 Alabugin I V, Manoharan M, Peabody S, et al. Electronic basis of improper hydrogen bonding: A subtle balance of hyperconjugation and rehybridization. J Am Chem Soc, 2003, 125: 5973－5987

20 Wlendening E D, Weinhold F. Natural resonance theory: I. general formalism. J Comp Chem, 1998, 19: 593－609

21 Bader R F W. Atom in Molecules－A Quantum Theory. Oxford: Oxford University Press, 1990

22 Bader R F W. A quantum theory of molecular structure and its applications. Chem Rev, 1991, 91: 893－928

23 Popelier P L A. Characterization of a dihydrogen bond on the basis of the electron density. J Phys Chem A, 1998, 102: 1873－1878